12

DEUTSCHE GESELLSCHAFT FÜR LUFT- UND RAUMFAHRT
LILIENTHAL-OBERTH E.V.

The interaction between oscillating panels and thin airlayers

W.M. Beltman and H. Tijdeman
University of Twente
The Netherlands

30 June 1998

On the interaction between oscillating panels and thin airlayers

W. M. Beltman and H. Tijdeman

University of Twente
Department of Mechanical Engineering
P .O. Box 217 7500 AE Enschede
The Netherlands

1. Introduction

A part of the research conducted by the Dynamics Group in Twente deals with the fluid-structure interaction between vibrating panels and thin layers of still air. This interaction is among other things of importance for the dynamical behaviour of solar panels, when folded as a package against the body of a satellite as happens during launch. Other examples concern the dynamical behaviour of panels backed by closed air cavities, of double-wall panels with an air- or fluidlayer in between and even the behaviour of piezo-electrically-activated printheads of inkjetprinters.

In order to investigate the mentioned interaction, exploratory measurements have been performed on rigid panels oscillating in pitch and heave. The panels were mounted parallel to a fixed surface. Subsequently measurements were performed on flexible panels backed by a cavity.

In parallel herewith theoretical results for rigid panels have been generated based on analytical solutions in closed form. For flexible panels a new finite element has been developed, which enables fully coupled calculations for complex geometries. The models include besides compressibility and inertia the effects of viscosity and heat conduction of the air.

It will be shown that the main parameter governing the motion of the air in narrow gaps is the so-called *shear wave number,* which is a measure for the ratio between inertial and viscous forces in the air. Other parameters of interest are the *reduced frequency* and the *narrowness* of the gap.

A very satisfactory agreement between the experimental and theoretical results is obtained. It is demonstrated that the interaction between structure and air gives rise to large changes in frequencies and mode shapes as a result of added mass- and stiffness effects of the air. In addition, it is possible to create a considerable amount of damping as a result of the viscous losses in the airgap. Under certain conditions even critical damping can be obtained.

In this paper emphasis is put on the physics and phenomena involved and it is shown that the addition of the new element provides a good design

tool for optimising solar array configurations and structures backed by gas- or fluid filled cavities.

2. Acousto-elastic coupling with inviscid air

2.1 Background

In acousto-elastic problems usually three types of modes are distinguished: *structural* modes, *acoustic* modes *and coupled (acousto-elastic)* modes. The structural modes are the modes of the structure in vacuum. The acoustic modes are the modes of the air in an enclosure when all walls are rigid and acoustically hard. For the coupled modes the mutual interaction between the vibrating structure and the air is taken into account. Of course, in practice we mostly have to deal with the latter type of modes. Especially in studies related to interior noise abatement in aircraft, cars etc.

Acousto-elastic problems nowadays can be handled reasonably well with most of the existing Finite Element Programs. Besides the elements describing the structure, acoustic elements are introduced together with provisions for the coupling between the structural and acoustic elements at the interface between structure and air. In most of the programs the air is represented as a compressible, inviscid medium and no mean flow. Its behaviour is described by the well-known wave equation (see figure 1).

The coupled set of finite element equations to be solved in case of full acousto-elastic coupling and the appropriate boundary conditions are given in figure 2.
At the interface between structure and air continuity of the velocity component normal to the surface is required. For acoustic hard walls zero normal velocity is demanded. For open boundaries the pressure release ($p = 0$) has to be imposed.

2.2. Validation

Experiments and calculations for an airtight box

To validate the inviscid acousto-elastic methods and to gain more insight into what happens physically, we repeated an experiment performed by Dowell, Gorman and Smith [1] in 1977. It concerned a rectangular airtight box with a flexible cover plate (figure 3). An aluminium plate, thickness 1 mm, was clamped in a thick-walled perspex box. By adjusting the position of the bottom the depth of the cavity could be varied. The eigenfrequencies and corresponding modeshapes were determined as a function of the cavity depth. The experimental set-up is depicted in figure 4. The plate was excited with an electrodynamic exciter and the response was determined with the help of accelerometers. Data acquisition, reduction and modal analysis took place with the LMS-CADA-X system.
Because of the difference in thermal expansion coefficients between aluminium and perspex the experiments had to be conducted under controlled climatic conditions.

The results of the measurements and the computations with the Finite Element Program ANSYS, shown together in figure 5, clearly demonstrate the large effect which a change in cavity depth has on the dynamical behaviour of the coverplate.

Physical Interpretation
In general a vibrating structure experiences the motion of the surrounding fluid as if it possesses an extra mass. For a plate vibrating in an unbounded air domain, exact solutions for the added mass are known [2]. In the present case, however, the air is trapped in a cavity. It turns out that for this situation two main effects can be distinguished: an added stiffness and an added mass effect. Moreover a third effect shows up, especially for narrow cavities, namely the presence of a considerable amount of damping.

Added stiffness
An added stiffness effect is present when the vibration of the plate is accompanied by a change of volume in the cavity, as sketched in figure 6. Due to the periodic compression and decompression, the cavity acts as a type of airspring. This effect, which occurs for symmetrical mode-shapes only, increases strongly with decreasing depth. Then the relative change in volume of the cavity increases, leading to a considerable increase in stiffness and thus in eigenfrequency.

Added mass
The added mass effect is important when the air in the cavity is 'pumped' back and forth under the action of the vibrating plate. This is, for instance, the case for the second mode shape as sketched in figure 7. As a result of the 'pumping' effect the plate experiences an added mass which increases with decreasing cavity depth. As a result the frequency drops.

Combined added mass and added stiffness effects
When the cavity depth is varied both aforementioned effects will occur simultaneously. This can be illustrated very well with the development of eigenfrequencies and mode shapes with cavity depth.

First mode (figure 8)
We follow the frequency curve as a function of cavity depth, starting at the largest depth. At first we note an increase in frequency up to about a depth of 30 mm. Thereafter the frequency slowly drops. Of interest is the accompanying change in mode shape: the mode shape gradually changes from a clear first bending mode to a different mode shape, with some resemblance to the third mode. The mode shape evidently tries to 'escape' volume changes. The added stiffness effect becomes smaller and a pumping effect takes over. Both effects are counteracting as is reflected in the behaviour of the eigenfrequency.

Second mode (figure 9)
Here we see that the shape of the second mode is hardly influenced by the depth of the cavity underneath. This is reflected in the development of the frequency with cavity depth. With decreasing depth the velocities of the air in the cavity will increase. The added mass increases as well and, as a result, the eigenfrequency drops continuously.

Third mode (figure 10)
Also for this mode a considerable change in mode shape occurs with decreasing cavity depth. For relatively large depths the added stiffness effect, connected with a change in volume, is about the same as the added mass effect, connected with the pumping effect. As a result the

frequency hardly changes. For more narrow cavities the mode shape has changed in such a way that the added stiffness effect becomes the dominating effect, resulting in an increase in frequency.
For a further decrease in depth (not shown in this figure; see also section 3.2.2) the added mass again becomes the dominating effect and the frequency drops.

Damping (figure 11)
The measurements on the airtight box also revealed the occurrence of extra damping, especially for the second mode and narrow cavities. This additional damping is to be attributed to viscous losses of the air in narrow gaps. These losses become largest for vibration modes, which create a substantial pumping effect.
It is evident that under these conditions the assumptions on which the wave equation is based are no longer valid.

The damping effect of narrow gaps is known from the literature [3 - 12]. A number of solutions are presented for very simple configurations (for an overview of the various methods reference is made to [13]) but a general method to compute the amount of damping for arbitrary shaped structures and cavities, including the full coupling, was missing. Because the available Finite Element Programs cannot handle this problem a new finite element has been developed and included in the B2000 program [13,15].

3. Acousto-elastic coupling including viscothermal effects

3.1. The low reduced frequency model

In order to capture also the damping effects as observed in the first set of measurements (figure 11) the acoustic model was extended with the effects of viscosity and thermal conductivity. The analysis (for details see [13]) is based on the linearised set of Navier-Stokes equations, the equation of continuity, the equation of state of an ideal gas and the energy equation. Under the following assumptions:

- small perturbations,
- no mean flow,
- depth of the gap small in comparison with the dimensions of the plate,
- velocity of the air normal to the plate negligible with respect to the in-plane velocities,

the low reduced frequency equation, shown in figure 12 is obtained.

The main parameters (figure 13) governing the problem are the so-called shear wave number, s, a measure for the ratio between inertial and viscous forces, and the reduced frequency k, a measure for ratio between the acoustic wave length and the depth of the gap.

It has been proved in [13] that this low reduced frequency equation suffices to solve the majority of problems associated with so-called squeeze film damping.

3.2. Application and validation

3.2.1 . Rigid panels oscillating normal to a fixed surface

Analytical solution
The modified wave equation has been solved first for rectangular, rigid panels, oscillating normal to a fixed surface [13,14]. Along the (open) side edges of the panel the condition $p = 0$ is imposed. The analytical solution is obtained for both heave and pitch motion. This enables -by linear combination- the determination of the air loads on rectangular panels for any rigid body motion normal to the fixed surface. This has some analogy with the way in which in the past unsteady forces and moments for flutter calculations were determined by using the two-dimensional unsteady aerodynamic coefficients for pitch and heave motions as sketched in figure 14 (see [17,18]).
The analytical solutions, representing the air loads felt by our panel are depicted in figures 15 and 16.
At this stage it has to be noted that the air loads working on oscillating panels in an unbounded domain are far less than the air loads felt by panels oscillating in the proximity of other panels or near a fixed wall. In the present case it was justified to discard the air loads working on the upper surface of the panel.

The solution [13] contains not only analytical expressions for the pressure distribution in the gap, but also of the temperature and velocity perturbations. As an illustration the in-plane velocity profile in the gap is given for different values of the shear wave number in figure 17. This figure clearly shows the transition from viscous flow (with a Poiseuille-type profile) for low values of the shear wave number to an inertia dominated flow (with an almost plane velocity profile) for high values of this parameter.

Experiments
As a first step experiments were performed on a rigid panel oscillating normal to a fixed bottom plate. This configuration was chosen to validate the low reduced frequency model on its own merits, not yet influenced by elastic deformations of the structure. For the experiments solar panels, provided by Fokker Space, were used, because such panels possess a very high stiffness to weight ratio. A lightweight panel is beneficial in order to have sufficient resolution to determine the reactions of the air on the oscillating panel. A stiff panel is required to avoid unwanted deformations.

The first set-up (figure 18) consisted of a panel suspended in eight springs (two at each corner) and hanging above a fixed surface. The depth of the air gap between the panel and bottom plate could be easily changed. Accelerometers were mounted on the panel to measure its response on the excitation and to verify the assumption of a rigid behaviour. By measuring the frequency and damping of this one-degree-of-freedom system for various positions of the bottom plate, the effects of a change in gap depth on the air loads have been determined.

It has to be stressed here that, because of the high damping values involved, it is essential to distinguish between the frequency at which

amplitude-resonance occurs and the so-called phase-resonance frequency, at which a phase shift of 90 degrees between excitation and response exists. The latter frequency corresponds with the eigenfrequency of the undamped system and has to be used when determining the virtual mass added by the reaction of the air.

In the second test set-up (figure 19) a panel was mounted in such a way that it could perform oscillations in pitch around mid-chord. Here in principle the same test procedure was applied.

The properties of the tested panels are collected in table 1.

TABLE 1 Properties of tested panels

	Panel I (Translation)		**Panel II (Rotation)**
Dimensions:	0.98 x 0.98 m		1.67 x 1.23 m
Mass:	2.516 kg	Moment of Inertia:	1.53 kg m^2
Springstiffness : (per spring)	1178 N/m		1959 N/m
Eigenfrequency: (in vacuum)	9.74 Hz		2.96 Hz
Shear wave number range:	1.9 - 100		1.9 - 55

Interpretation of results and comparison between theory and experiment

From the calculated and experimental results for the panel oscillating in translation, collected in figures 20 and 21, it can be learned that the eigenfrequency strongly decreases with decreasing gap depth. At the same time the damping strongly increases. In the narrow gap a strong pumping effect is created, because the air is moving in and out the gap during each cycle of vibration. This results in a considerable amount of added mass and a substantial amount of damping. To give some numbers: for a gap of 3 mm the damping becomes almost critical and the added mass amounts 20 kg, for a net weight of the panel of only 2.5 kg.

Similar findings apply for the panel oscillating around mid-chord. The results in figures 22 and 23 reveal again a considerable effect of the thin air layer on as well eigenfrequency as on damping. In this case the shift in eigenfrequency is the result of an added mass moment of inertia. The mass moment of inertia of the panel itself is 1.5 kg m^2. For a gap of 3 mm, the air causes an additional moment of inertia of 5.5 kg m^2.

Evidently, we have to deal with complex numbers, a situation not uncommon for aeroelasticians. Of course the origin of the 'complexity' is completely different: viscous effects in a thin airlayer (without mean flow) versus a periodic change in circulation around an airfoil oscillating in an air stream.

The results presented so far (figures 20 to 23) show a satisfactory agreement between calculated and measured results, which justifies the conclusion that the low reduced frequency model is well suited for the prediction of the unsteady behaviour of the flow in narrow gaps.

3.2.2. Flexible coverplate on an airtight box

numerical solution
The theory described in the preceding section can be used to calculate the interaction between a flexible structure and a thin layer of air. Analytical solutions for this interaction problem can only be obtained for simple configurations. In order to be able to model the interaction for more complex geometries, a new finite element was implemented in the finite element program B2000. This element includes the effects of viscosity and heat conduction (for details see [13,15]). By demanding continuity of (normal) velocity at the interface between structure and air again a fully coupled acousto-elastic finite element formulation is obtained (figure 24). The resulting system of equations is complex, asymmetric and frequency dependent.

Experimental validation
With the object to validate the finite element formulation, we repeated the tests described in section 2.2. This time an all aluminium frame was used to avoid temperature effects caused by the differences in thermal expansion coefficients. The width of the plate was 245 mm, slightly less than the 250 mm wide plate used in the earlier test.

The development of the lowest seven eigenfrequencies of the cover plate is presented in figure 25. As could be expected a large effect of the air in the gap on the vibration characteristics is found, which increases with decreasing depth. This is especially true for modes 1.1, 2.1 and 3.1. These results demonstrate that an accurate prediction of the dynamic behaviour of flexible panels connected with narrow gaps can only be achieved if the interaction is fully taken into account.
Again, it can be observed that also the modes change their shapes drastically with decreasing gap depth (figure 26). It looks as if for very narrow gaps the mode shapes try to escape changes of volume in the cavity.

The development of the damping of mode 1.1 and 2.1 with gap depth (figure 27) confirms that a considerable amount of damping can be created, provided that the mode shapes generate sufficient pumping of the air in the gap.

The comparison between the results of the experiments and the computed results is quite satisfactory. In other words, we now have developed a new tool to design structures that may benefit or suffer from the presence of narrow gaps or cavities.

4. Engineering applications

The first application (figure 28) of the presented method deals with the dynamic behaviour of solar panels, folded against the satellite with thin air layers in between (before and during launch). The program has been applied in studies performed in collaboration with Fokker Space [16]. In addition, experiments have been conducted to determine the effect of barriers (cables etc.) in the gaps [13].

A second application concerns the design of smart walls, which vibrate in such a way that in a specified frequency range a maximum of energy is dissipated. An investigation, under contract with the Dutch Technology Association (STW) is underway.

Finally, the method is incorporated in the design process of piezo-electrically-driven printheads of inkjetprinters. Here, the knowledge about the interaction between the activated piezo, the ink in the ink-channel and the flexible structure is essential to produce inkdrops on the right time in the right place.

5. Concluding remarks

In a systematic approach an engineering tool has been developed and validated to handle structures in which squeeze film damping plays an essential role. Its value has been demonstrated with a number of engineering applications.

6. Acknowledgements

This paper contains an overview of recent work performed by the Dynamics Group in the faculty of Mechanical Engineering in Twente, which besides the authors consists of T.G.H. Basten, F.J.M. van der Eerden, P.J.M. van der Hoogt, R.M.E.J. Spiering and A.G.M. Wolbert. In addition, a number of MSc-students contributed to the presented work.
The program is performed under contract with the Dutch Technology Foundation (STW). Shell contributed to the procurement of instrumentation for vibration testing.

7. References

1 Dowell, E.H., Gorman, F., Smith, D.A., *Acousto-elasticity: general theory, acoustic natural modes to sinusoidal excitation, including comparisons with experiment,* Journal of Sound and Vibration, Vol.52, p.519 - 542, 1977.

2 Blevins, R.D., *Formula for natural frequency and modeshape,* Van Nostrand Reinholds Company, New York, 1979.

3 Trochidis, A., *Körperschalldampfung durch Viscositätsverluste in Gasschichten bei Doppelplatten,* PhD-thesis, ITA Berlin, 1977.

4 Trochidis, A., *Vibration damping due to air- or liquid layers,* Acustica, Vol.51, p.201 - 212, 1982.

5 Fox, M.J.H., Whitton, P.N., *The damping of structural vibrations by thin gas films,* Journal of Sound and Vibration, Vol.73(2),p.279 - 295,1980.

6 Möser, M., *Damping of structure born sound by the viscosity of a layer between two plates,* Acustica, Vol.46, p.210 - 217, 1980.

7 Moldover, M., Mehl, J., Greenspan, M., *Gasfilled spherical resonators: Theory and Experiment,* Journal of the Acoustic Society of America, Vol.79, p.253 - 270, 1986.

8 Bruneau, M., Herzog, Ph., Kergomard, J., Polack, J.D., *General formulation of the dispersion equation in bounded visco-thermal fluid,* Wave Motion, Vol.11, p.441 - 451, 1989.

9 Chow, L.C., Pinnington, R.J., *Practical industrial method of increasing structural damping in machinery, I. Squeeze film damping with air,* Journal of Sound and Vibration, Vol. 118, p.123 - 139, 1989.

10 Chow, L.C., Pinnington, R.J., *Practical industrial method of increasing structural damping in machinery, II. Squeeze film damping with liquids,* Journal of Sound and Vibration, Vol. 128, p.333 - 347, 1989.
11 Önsay, T., *Effect of layerthickness on the vibration response of a plate - fluid layer system,* Journal of Sound and Vibration, Vol.163, p.231 - 259, 1993.
12 Karra, C., Ben Tahar, M., *An integral equation formulation for boundary element analysis of sound propagation in viscothermal fluids,* Journal of the Acoustic Society of America, Vol.103(3), p.1311-1318, 1997.
13 Beltman, W.M., *Viscothermal wave propagation including acousto-elastic interaction,* PhD - Thesis, to appear october 1998.
14 Beltman, W.M., Van der Hoogt, P.J.M., Spiering, R.M.E.J., Tijdeman, H., *Air loads on a rigid panel oscillating normal to a fixed surface,* Journal of Sound and Vibration, Vol. 206(3),p. 217 - 241, 1997.
15 Beltman, W.M., Van der Hoogt, P.J.M., Spiering, R.M.E.J., Tijdeman, H.,*Implementation and experimental validation of a new viscothermal acoustic finite element for acousto-elastic problems,* Journal of Sound and Vibration, to appear in 1998.
16 Beltman, W.M., Van der Hoogt, P.J.M., Spiering, R.M.E.J., Tijdeman, H., *Air loads on solar panels during launch,* ESA SP-386, p.219 - 226, Conference on Spacecraft structures, materials and mechanical testing, ed. Burke, W.R., Noordwijk, 1996.
17 Försching, H., Grundlagen der Aeroelastik, Springer, 1974
18 Anonymus, AGARD Manual on Aeroelasticity, Vol.VI, 1968.

Fig 1: Wave equation with appropriate boundary conditions

$$\nabla^2 p + \left(\frac{\omega}{c_0}\right)^2 p = 0$$

$$\begin{aligned}
\frac{\partial p}{\partial n} = 0 \quad &: \quad \text{zero velocity} \\
Z_n \frac{\partial p}{\partial n} = -i\left(\frac{\omega}{c_0}\right) p \quad &: \quad \text{impedance condition} \\
\frac{\partial p}{\partial n} = \omega^2 u_{sn} \quad &: \quad \text{coupling with vibrating structure} \\
p = 0 \quad &: \quad \text{pressure release}
\end{aligned}$$

- standard acoustic: inviscid, adiabatic, small disturbances

Fig 2: Standard acoustic finite element formulation

$$-\omega^2 \begin{bmatrix} [M^s] & [0] \\ [M^c] & [M^a] \end{bmatrix} \begin{Bmatrix} \{U\} \\ \{P\} \end{Bmatrix} + \begin{bmatrix} [K^s] & -[K^c] \\ [0] & [K^a] \end{bmatrix} \begin{Bmatrix} \{U\} \\ \{P\} \end{Bmatrix} = \begin{Bmatrix} \{F^{ext}\} \\ \{0\} \end{Bmatrix}$$

- $[M^s]$, $[K^s]$: structural mass and stiffness matrices
- $[M^a]$, $[K^a]$: acoustic mass and stiffness matrices
- $[M^c]$, $[K^c]$: coupling matrices
- $\{U\}$, $\{P\}$: structural and acoustic degrees of freedom

Fig 3: Rigid box with flexible coverplate [1]

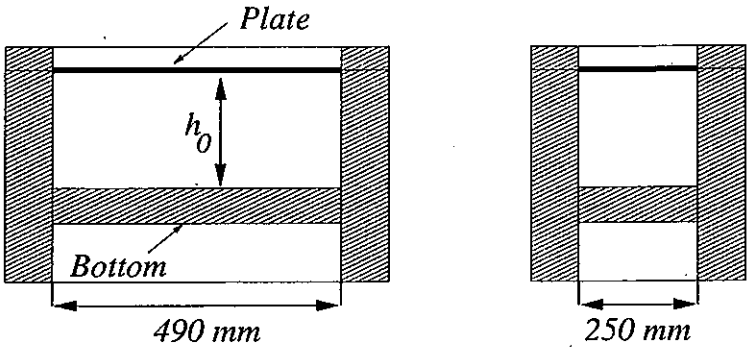

$t_p = 1$ mm
Aluminum
5 mm $< h_0 <$ 266 mm

- Eigenfrequencies and modes shapes as a function of h_0
- Comparison with FEM results

Fig 4: Experimental setup

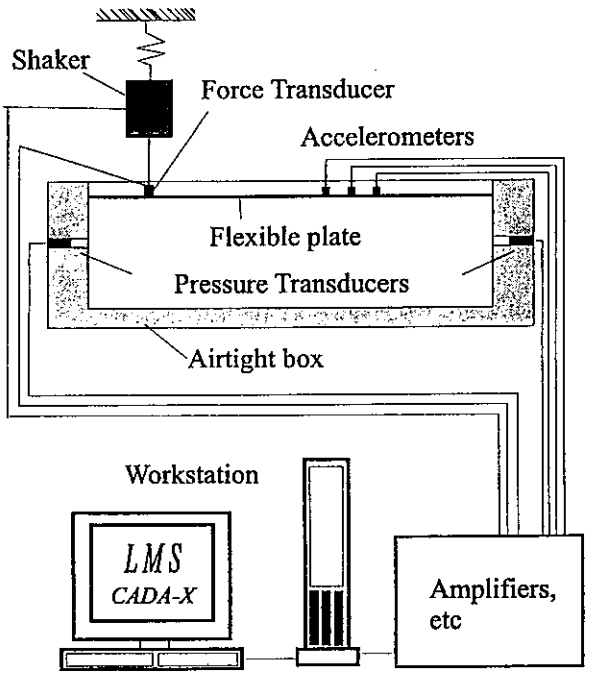

Fig 5: Eigenfrequencies versus depth and mode shapes in vacuum

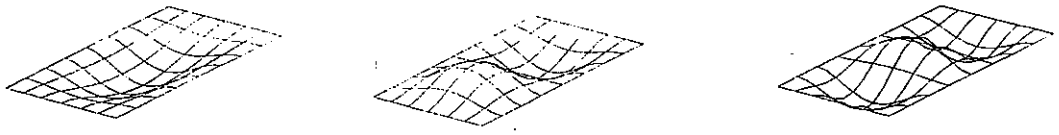

Acousto-elastic modes:

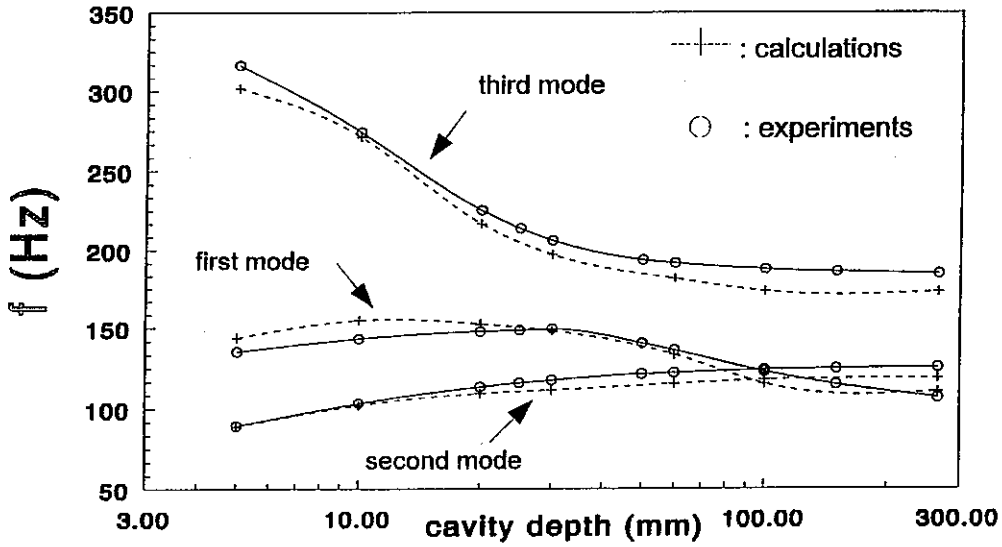

Fig 6: Added stiffness, volume change

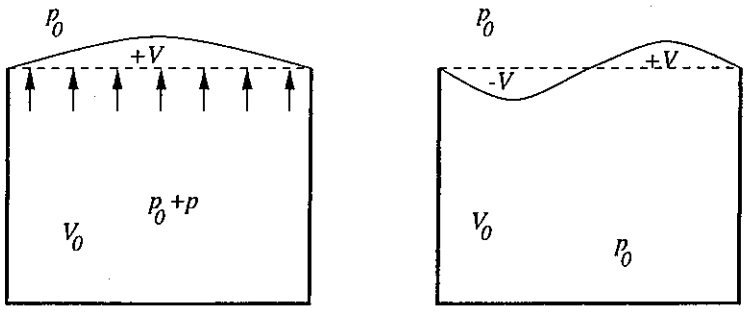

Net volume change

No net volume change

Fig 7: Added mass, pumping effect

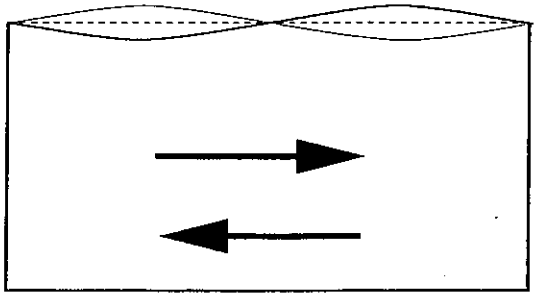

Fig 8: Physical interpretation mode 1: frequency and mode shape

First mode:

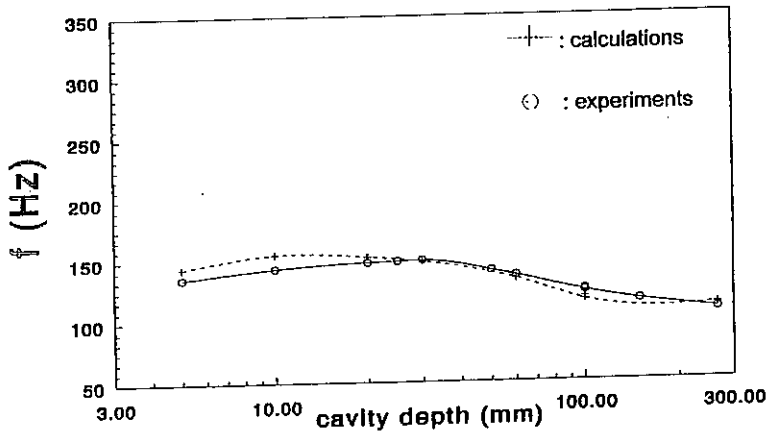

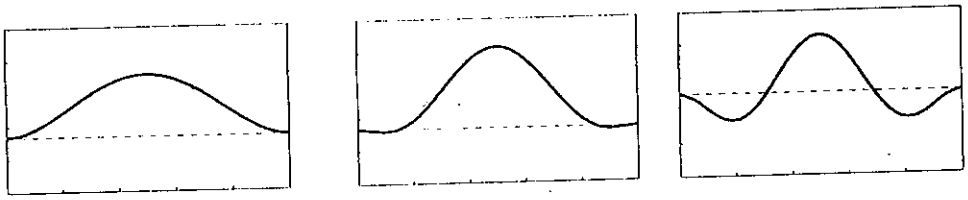

depth = 266 mm

depth = 50 mm

depth = 10 mm

Fig 9: Physical interpretation mode 2: frequency and mode shape

Second mode:

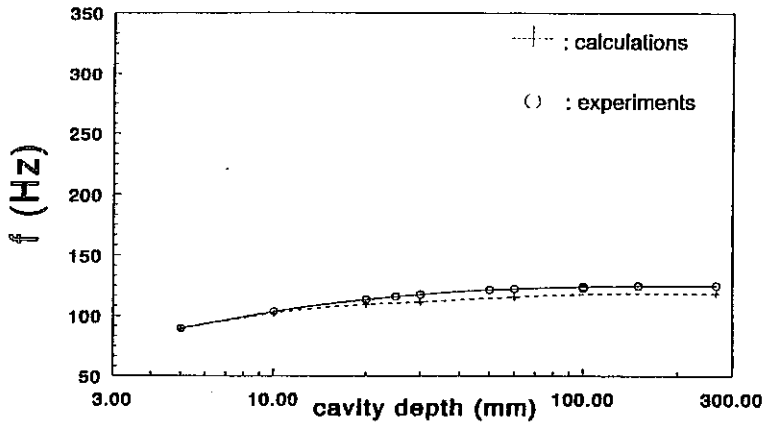

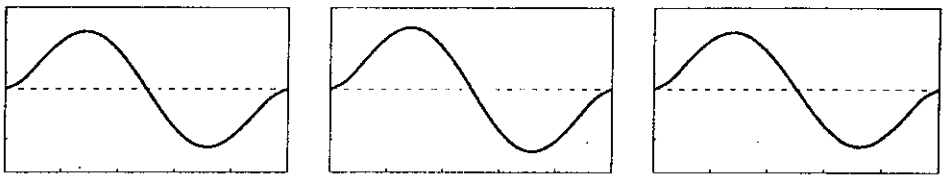

depth = 266 mm depth = 50 mm depth = 10 mm

Fig 10: Physical interpretation mode 3: frequency and mode shape

Third mode:

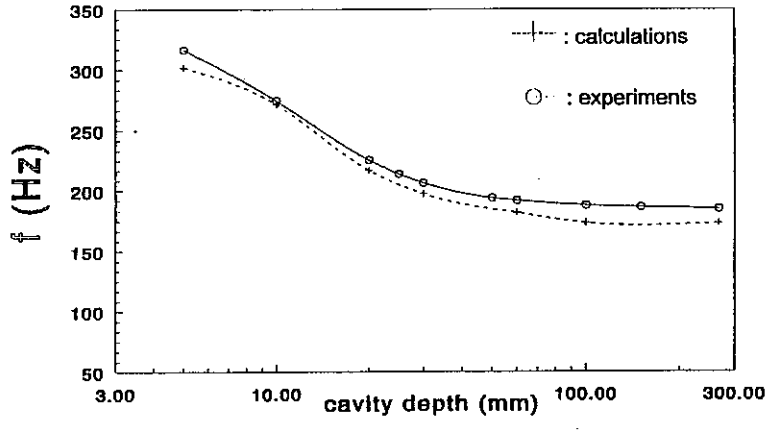

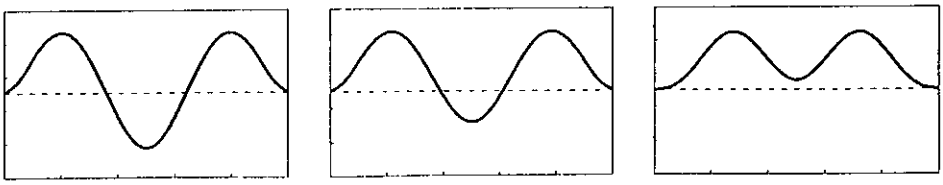

depth = 266 mm depth = 50 mm depth = 10 mm

Fig 11: Damping versus depth

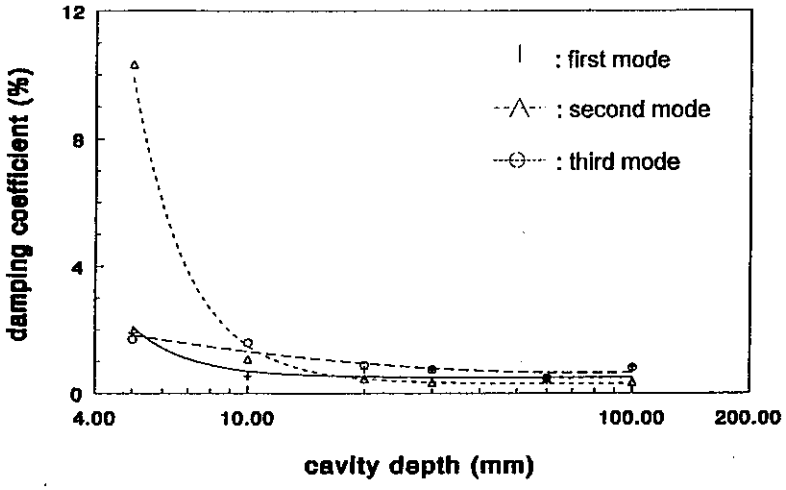

Fig 12: Low reduced frequency equation

$$\frac{\partial^2 p}{\partial x^2} + \frac{\partial^2 p}{\partial y^2} - \frac{\omega^2 \Gamma^2}{c_0^2} p = -\frac{\rho_0 \omega^2}{B(s)} h(x, y)$$

- Propagation constant Γ includes viscous and thermal effects
- $B(s)$ due to viscous effects
- Source term due to squeeze motion of surfaces
- New acousto-elastic finite element model

Fig 13: Main parameters governing the low reduced frequency model

$$s = h_0\sqrt{\frac{\rho_0\omega}{\mu}} \quad ; \quad k = \frac{\omega h_0}{c_0}$$

- s: ratio between inertial forces and viscous forces
- k: ratio between gap width and acoustic wave length
- low reduced frequency model: $k \ll 1$ and $k/s \ll 1$

Fig 14: Rotation around arbitrary axis, split-up

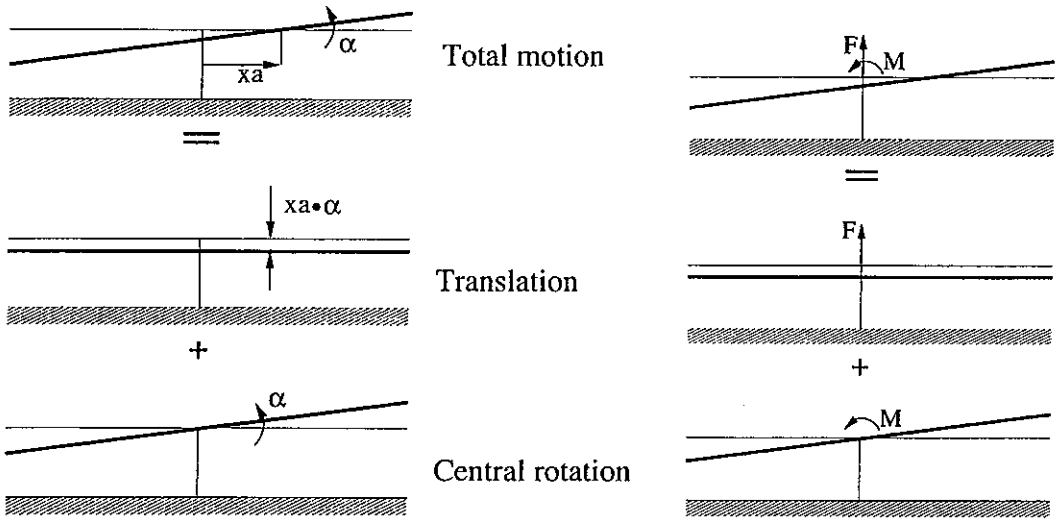

Fig 15: Aerodynamic coefficients (dimensionless coordinates $-1 \leq xa \leq 1$)

$$F_{\frac{1}{4}} = 2\pi\rho_0 l_x^3 l_y \left[k_a\left(xa - \frac{1}{2}\right) + k_b\right]\alpha\omega^2$$

$$M_{\frac{1}{4}} = -2\pi\rho_0 l_x^3 l_y \left[m_a\left(xa - \frac{1}{2}\right) + m_b\right]\alpha\omega^2$$

Fig 16: Viscothermal aerodynamic coefficients

$$k_a = \frac{16a^2}{\pi^3 B(s) g} \sum_{q=1,3\cdots}^{\infty} \frac{1}{q^2 D^2}\left[1 - \frac{\tanh(D)}{D}\right]$$

$$m_a = k_b = \frac{1}{2}k_a$$

$$m_b = \frac{16a^2}{\pi^3 B(s) g} \sum_{q=2,4\cdots}^{\infty} \frac{1}{q^2 D^2}\left[1 - \frac{\tanh(D)}{D}\right] - \frac{1}{4}k_a$$

- a: aspect ratio, g: narrowness of gap, B(s): viscosity function
- $D = \sqrt{\left(\frac{q\pi}{2a}\right)^2 - \frac{k^2\gamma a^2}{nB(s)g^2}}$
- n: polytropic constant
- Viscothermal effects included: complex air loads in still air

Fig 17: Velocity profile in the gap for different shear wave numbers:

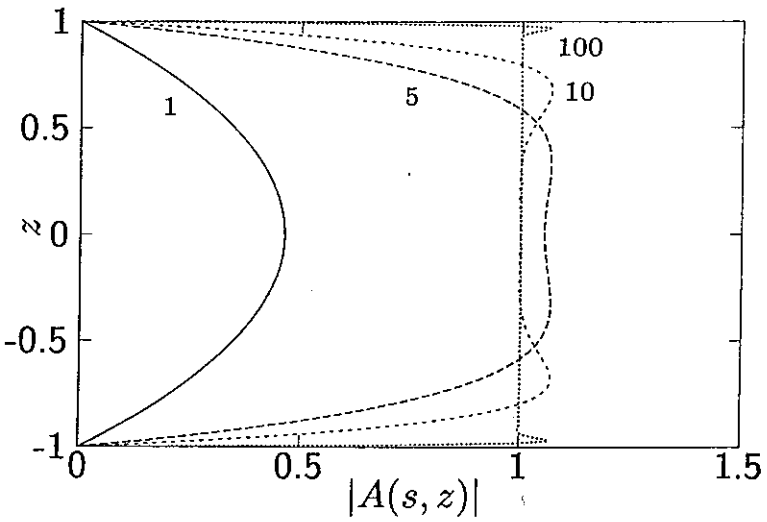

Fig 18: Translating rigid solar panel: 0.98 x 0.98 m , 2.5 kg, SDOF system

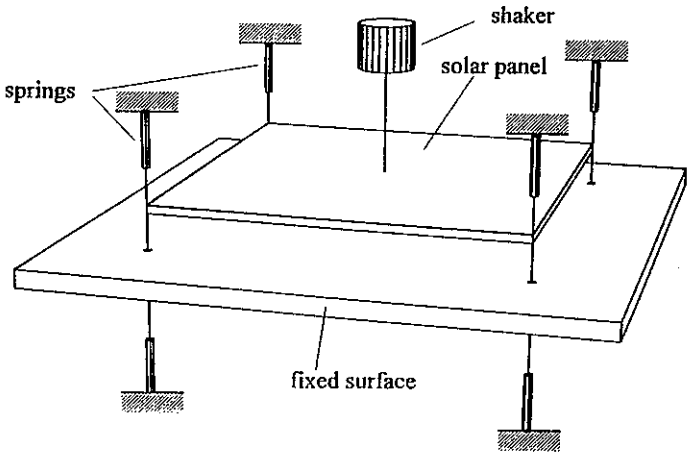

Fig 19: Rigid solar panel rotating around central axis: 1.67 x 1.29 m

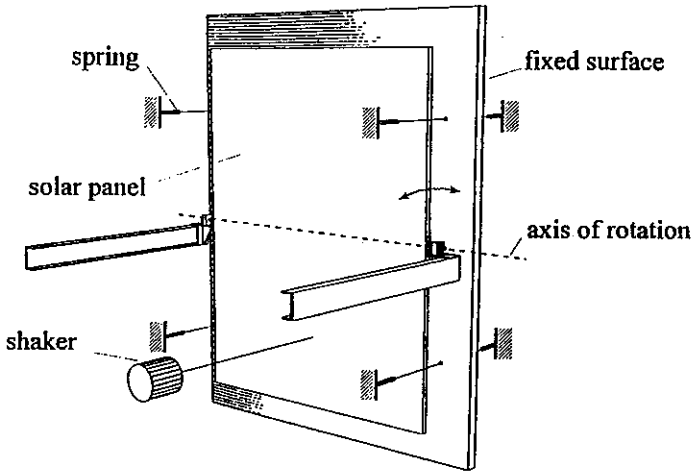

Fig 20: Eigenfrequency versus depth translating panel

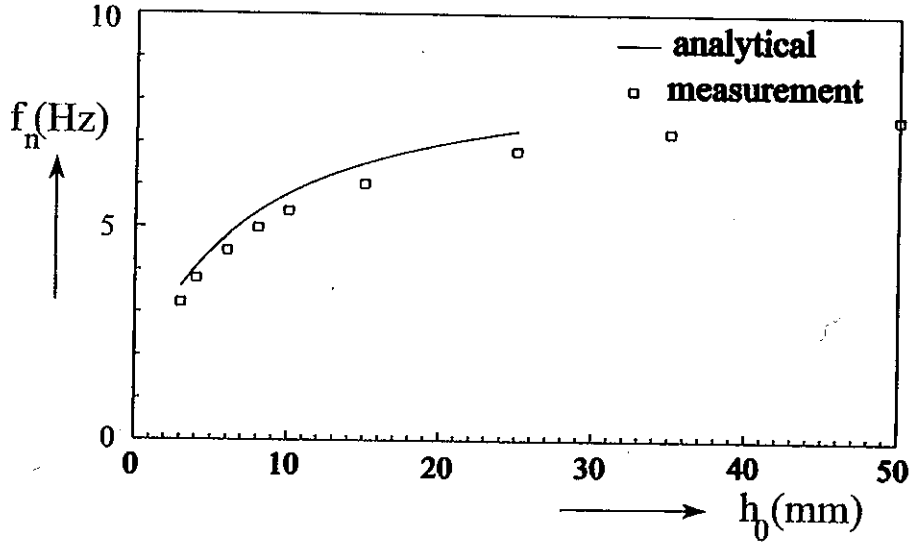

Fig 21: Damping versus depth translating panel

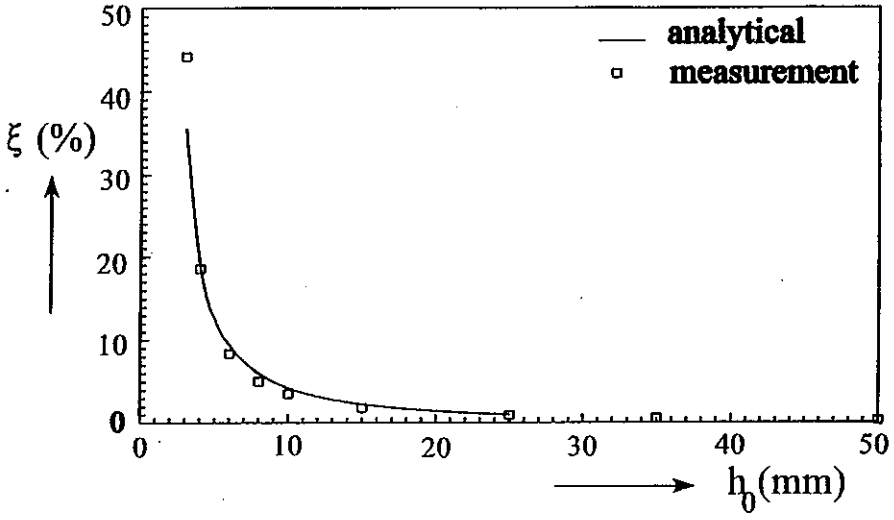

Fig 22: Eigenfrequency versus depth rotating panel

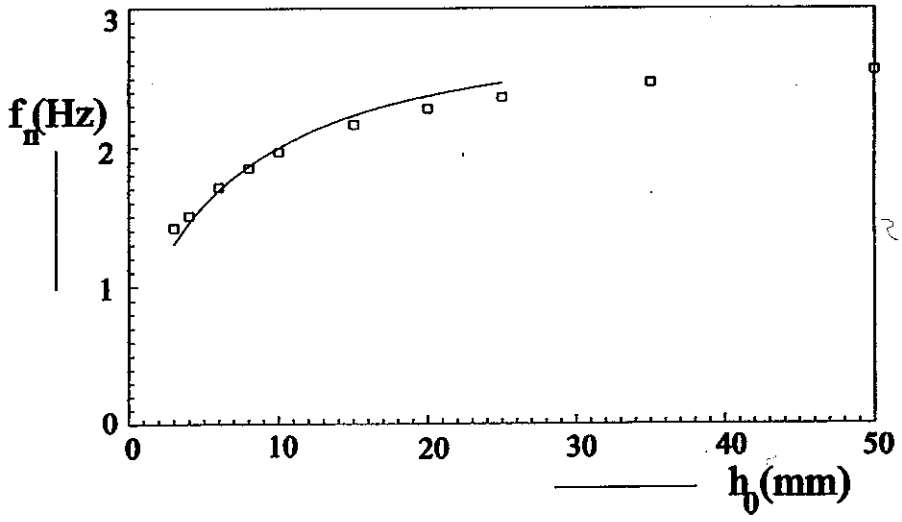

Fig 23: Damping versus depth rotating panel

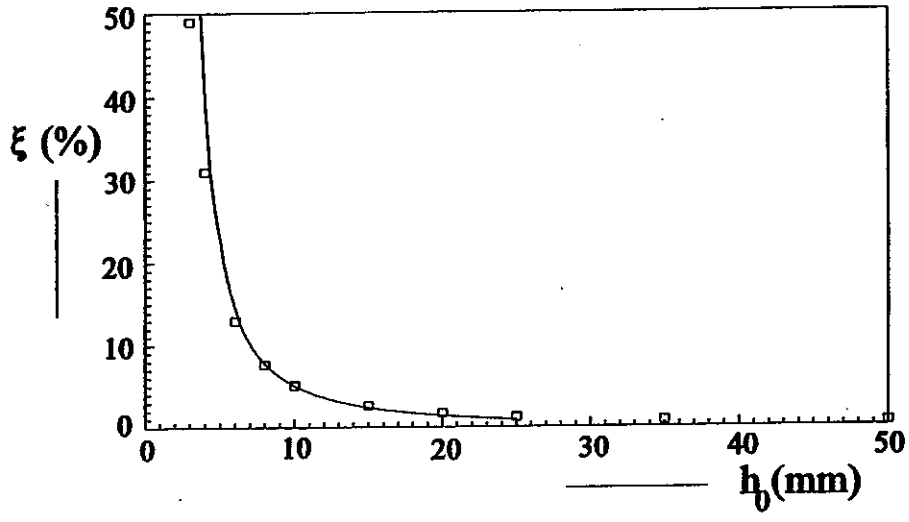

Fig 24: Viscothermal acousto-elastic finite element model

$$-\omega^2 \begin{bmatrix} [M^s] & [0] \\ [\hat{M}^c] & [\hat{M}^a] \end{bmatrix} \begin{Bmatrix} \{U\} \\ \{P\} \end{Bmatrix} + \begin{bmatrix} [K^s] & -[K^c] \\ [0] & [\hat{K}^a] \end{bmatrix} \begin{Bmatrix} \{U\} \\ \{P\} \end{Bmatrix} = \begin{Bmatrix} \{F^{ext}\} \\ \{0\} \end{Bmatrix}$$

- $[M^s]$, $[K^s]$: structural mass and stiffness matrices
- $[\hat{M}^a]$, $[\hat{K}^a]$: viscothermal acoustic mass and stiffness matrices
- $[\hat{M}^c]$, $[K^c]$: coupling matrices
- $\{U\}$, $\{P\}$: structural and acoustic degrees of freedom
- complex, frequency dependent matrices
- 2-D elements

Fig 25: Eigenfrequency versus depth

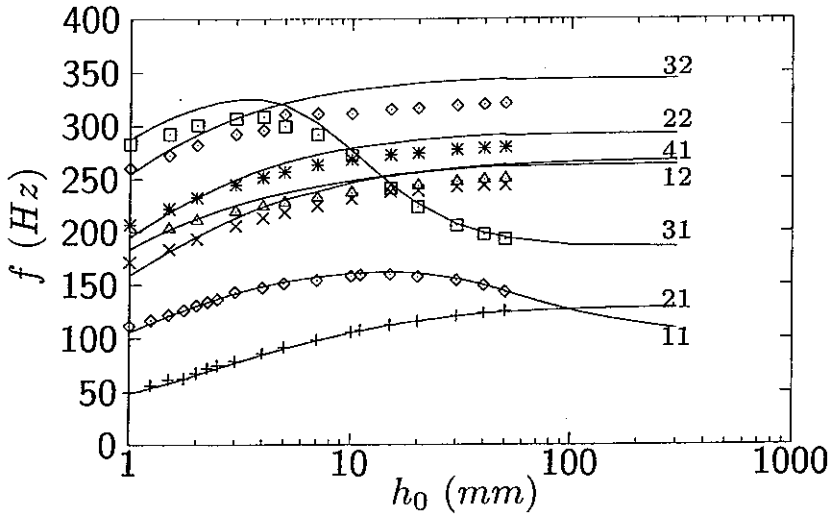

Fig 26: Mode shapes that change as function of depth

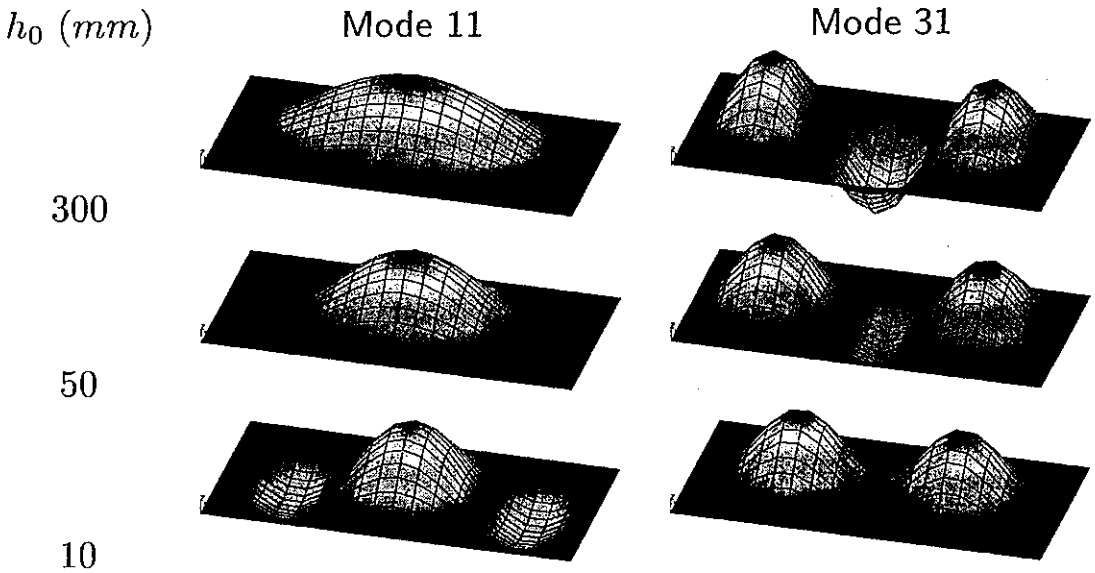

Fig 27: Damping versus depth

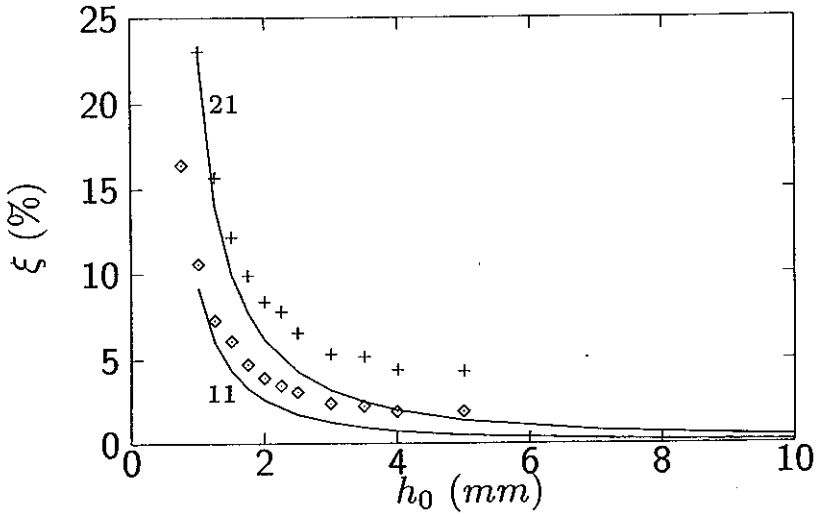

Fig 28: Engineering applications

- behaviour of stacked solar panels during launch

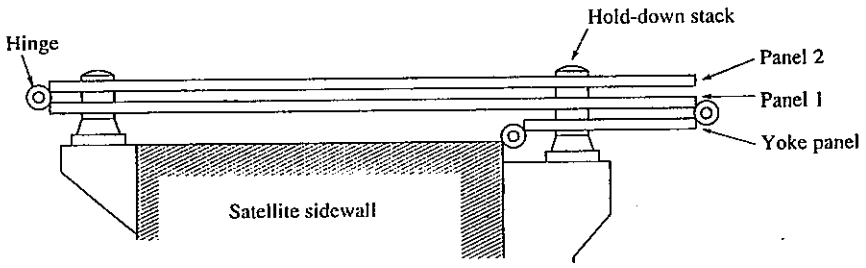

- behaviour of inkjet head

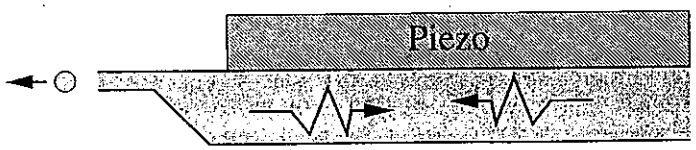

- damping of double wall panels